

Quantum Black Holes and their Lepton Signatures at the LHC with CalCHEP

Alexander Belyaev^{1,2,*} and Xavier Calmet^{3,†}

¹*School of Physics and Astronomy, University of Southampton, Highfield, Southampton SO17 1BJ, UK*

²*Particle Physics Department, Rutherford Appleton Laboratory, Chilton, Didcot, Oxon OX11 0QX, UK.*

³*Physics and Astronomy, University of Sussex, Falmer, Brighton, BN1 9QH, UK*

We discuss a field theoretical framework to describe the interactions of non-thermal quantum black holes (QBHs) with particles of the Standard Model. We propose a non-local Lagrangian to describe the production of these QBHs which is designed to reproduce the geometrical cross section πr_s^2 for black hole production where r_s is the Schwarzschild radius. This model is implemented into CalCHEP package and is publicly available at the High Energy Model Database (HEPMDB) for simulation of QBH events at the LHC and future colliders. We present the first phenomenological application of the QBH@HEPMDB model with spin-0 neutral QBH giving rise the e^+e^- and $e\mu$ signatures at the LHC@8TeV and LHC@13TeV and produce the respective projections for the LHC in terms of limits on the reduced Planck mass, \overline{M}_{PL} and the number of the extra-dimensions n .

*Electronic address: a.belyaev@soton.ac.uk

†Electronic address: x.calmet@sussex.ac.uk

I. INTRODUCTION AND MODEL SETUP

Realising that the Planck mass [1–5] may not be around 10^{19} GeV but that it is a model dependent quantity which could even be as low as a few TeVs has had a considerable impact in particle physics. One of the most amazing signatures of these models would be the creation of small black holes at colliders [6–10] or in the scattering of cosmic rays [11–18] in the upper atmosphere of our planet. While it is now well appreciated that semi-classical black holes cannot be produced at the LHC because this collider is not energetic enough even if the Planck mass is at a few TeVs [19], the possibility remains to produce non-thermal quantum black holes [10].

While the semi-classical black holes, which have been extensively studied [6–9, 11–14, 18, 20–22], have masses between 5 to 20 times larger than the Planck scale and are thus thermal objects, most quantum black holes are those with masses of the order of the Planck scale. They will thus be non-thermal objects and their decomposition is thus not expected to be well described by Hawking radiation. They will rather explode into just a few particles resembling strong gravitational re-scattering. It is thus tempting to treat them as particles with a mass and carrying the quantum numbers of the particles which created them. In a proton collider, there will be quarks and gluons. The aim of this paper is to extend the work presented in [23] where a field theoretical model to describe the interactions of non-thermal quantum black holes with the particles of the standard model was proposed. This framework assumes that quantum black holes can be treated as quantum fields, i.e. they are classified according to representations of the Lorentz group. Furthermore, they are classified according to their transformations under the gauge groups of the standard model. This fixes their interactions with matter.

In a proton-proton collider, quantum black holes would be produced from the collisions of quarks and gluons if the Planck scale is low enough. We are thus particularly interested in the quantum black holes carrying QCD and QED quantum numbers and with spins 0, 1/2 and 1 since these should be the lowest lying states. We shall treat the mass spectrum as being discrete. Generically speaking, quantum black holes form representations of $SU(3)_c$ and carry a QED charge. The process of two partons p_i, p_j forming a quantum black hole in the c representation of $SU(3)_c$ and charge q as: $p_i + p_j \rightarrow \text{QBH}_c^q$ is considered in [10]. The following different transitions are possible at a proton collider:

$$\text{a) } \mathbf{3} \times \bar{\mathbf{3}} = \mathbf{8} + \mathbf{1}$$

$$\text{b) } \mathbf{3} \times \mathbf{3} = \mathbf{6} + \bar{\mathbf{3}}$$

$$\text{c) } \mathbf{3} \times \mathbf{8} = \mathbf{3} + \bar{\mathbf{6}} + \mathbf{15}$$

$$\text{d) } \mathbf{8} \times \mathbf{8} = \mathbf{1}_S + \mathbf{8}_S + \mathbf{8}_A + \mathbf{10} + \bar{\mathbf{10}}_A + \mathbf{27}_S$$

Most of the time the black holes which are created carry a $SU(3)_c$ charge and come in different representations of $SU(3)_c$ as well as QED charges. This allows the prediction of how they will be produced or decay. The aim of this work is to propose a framework to describe these interactions. We shall assume that the cross section for quantum black holes can be extrapolated from the classical and semi-classical cases, i.e. that it is given by the geometrical formula (see e.g. [20, 21])

$$\sigma = \pi r_s^2 \tag{1}$$

where r_s is the four-dimensional Schwarzschild radius

$$r_s(s, \bar{M}_{PL}) = \frac{\sqrt{s}}{4\pi \bar{M}_{PL}^2}, \tag{2}$$

where s is the invariant mass of the colliding particles, which upon exceeding the reduced Planck mass, \bar{M}_{PL} creates the respective QBH. Therefore, in terms of s and \bar{M}_{PL} , the cross section of the QBH production takes a form

$$\sigma = \frac{1}{16\pi} \frac{s}{\bar{M}_{PL}^4} \Theta(\sqrt{s} - \bar{M}_{PL}) \tag{3}$$

where we have assumed that the threshold mass for quantum black holes is identified with the Planck mass. Note that the quantum black holes described here are assumed to have a continuous mass spectrum despite some indications that their mass spectrum could be discrete [24]. Since we are considering a continuous mass spectrum we have to assume that quantum black hole couplings to long wavelength and highly off-shell perturbative modes are suppressed

[10]. Otherwise their contribution to low energy observables such as K_L decays would have been noticed a long time ago. Note that there are no such constraints if the mass spectrum of quantum black holes is indeed discrete [25].

We shall first reconsider the production of spinless quantum black holes in the collisions of two fermions (quarks for example with the appropriate colour factor). We start with the Lagrangian

$$L_{fermion+fermion} = \frac{c}{\overline{M}_{PL}^2} \partial_\mu \partial^\mu \phi \bar{\psi}_1 \psi_2 + h.c. \quad (4)$$

where c is the (non-local) parameter we will use to match the semiclassical cross section, \overline{M}_{PL} is the reduced Planck mass, ϕ is a scalar field representing the quantum black hole, and ψ_i is a fermion field. The cross section for ϕ production is:

$$\sigma(2\psi \rightarrow \phi) = \frac{\pi}{s} |A|^2 \delta(s - M_{BH}^2) \quad (5)$$

where M_{BH} is the mass of the black hole, $s = (p_1 + p_2)^2$ and p_1, p_2 are the four-momenta of ψ_1, ψ_2 . We find

$$|A|^2 = s^2 \frac{c^2}{\overline{M}_{PL}^4} [s - (m_1 + m_2)^2] \quad (6)$$

where m_1 and m_2 are the masses of the fermions ψ_1 and ψ_2 . We now compare this cross section with the geometrical cross section. If we use the representation for the delta-function written in the form of the Poisson kernel,

$$\delta(s - M_{BH}^2) = \frac{\Gamma M_{BH}}{\pi[(s - M_{BH}^2)^2 + \Gamma^2 M_{BH}^2]} \quad (7)$$

where Γ is the decay width of ϕ , we find:

$$c^2 = \frac{9}{4} \frac{4s^{\frac{3}{2}} - 8sM_{BH} + 4\sqrt{s}M_{BH}^2 + \sqrt{s}\Gamma^2}{\Gamma\pi[s - (m_1 + m_2)^2]} \quad (8)$$

Finally Γ can be calculated using the Lagrangian (4) as:

$$\Gamma = \frac{c^2}{8\pi} \frac{M_{BH} \sqrt{(M_{BH}^2 - (m_1 + m_2)^2)(M_{BH}^2 - (m_1 - m_2)^2)}}{\overline{M}_{PL}^4} \quad (9)$$

We can thus find an expression for our non-local parameter c by inserting Γ into the expression for c (8). In the case $m_1 = m_2 = 0$, one has a remarkably simple expression:

$$c^2 = \frac{8\pi \overline{M}_{PL}^4 (s - M_{BH}^2)}{M_{BH}^3 \sqrt{128\pi^2 \overline{M}_{PL}^4 s - M_{BH}^6}} \quad (10)$$

One can see that non-local behaviour of the c -coupling is quite non-trivial – it actually compensates the Breit-Wigner behaviour of the squared matrix element which would appear in case of constant c and leads to the expected s -dependence of the cross section from Eq.(3). It is important to realize that the QBH does not appear as a resonance since its parton level cross section is constructed to reproduce the semi-classical cross section as a function of s . With this in mind, we have also found an alternative approach to the construction of the QBH Lagrangian. If we recall that the Lagrangian for the four-fermion interactions

$$\mathcal{L}_{cont} = \frac{g_c}{\Lambda^2} \bar{\psi}_i \psi_i \bar{\psi}_j \psi_j \quad (11)$$

provides the squared matrix element for $\bar{\psi}_i \psi_i \rightarrow \bar{\psi}_j \psi_j$ scattering,

$$|M|^2 = \frac{g_c^2}{\Lambda^4} \quad (12)$$

and the respective total $\bar{\psi}_i \psi_i \rightarrow \bar{\psi}_j \psi_j$ cross section (neglecting the fermion masses)

$$\sigma = \frac{1}{16\pi s} |M|^2 = \frac{g_c^2}{16\pi} \frac{s}{\Lambda^4}, \quad (13)$$

then after comparison with Eq.(3), we can immediately see that Eq.(3) can be reproduced by 4-fermion interactions with $g_c = 1$ and $\Lambda = \overline{M}_{PL}$. In case of different fermion species involved in $2 \rightarrow 2$ process of the QBH production and decay, g_c will include the respective number of degrees of freedom to correctly reproduce the QBH branching fractions. In the scenario under study we consider the case of spin-0 neutral QBH production which preserves $SU(3) \times SU(2) \times U(1)$ gauge invariance but does not conserve flavour. We wish to emphasise that we are here only considering colourless quantum black holes which explains why our branching ratios are different from those of [3] (see also [26]). We have found that the most elegant and practical way to express these contact interactions is to use the auxiliary, non propagating scalar field, X which enters the following Lagrangian

$$\mathcal{L}_{cont}^X = g_c \left(\sum_{leptons} \bar{\psi}_i^\ell \psi_j^\ell X + \sum_{quarks} \bar{\psi}_i^q \psi_j^q X \right), \quad (14)$$

where i, j are lepton and quark flavour indices, propagator of “contact” X field is $\frac{i}{\overline{M}_{PL}^2}$, $g_c = (n_l + 3n_q)^{-1/4}$ is the normalisation factor accounting number of lepton, $n_l = 9$ and quark, $n_q = 18$ combinations, including the quark colour factor. This Lagrangian exactly reproduces the cross section of the spinless neutral QBH production and decay in the $2 \rightarrow 2$ fermion process as a function of s at the parton level (up to the multiplicative trivial form-factor $FF = \Theta(\sqrt{s} - \overline{M}_{PL})$).

Our results could be generalised easily to the case of initial state particles with different spins and colours for which the approach of the contact interactions also works successfully as one can check using dimensional analysis approach.

The result can be also generalised to the case of higher dimensional quantum black holes for which the Schwarzschild radius is given by (see e.g. [6])

$$r_s(s, n, \overline{M}_{PL}) = k(n) \overline{M}_{PL}^{-1} (\sqrt{s} / \overline{M}_{PL})^{1/(1+n)} \quad (15)$$

where n is the number of extra-dimensions, \overline{M}_{PL} the $4+n$ reduced Planck mass and $k(n)$ reads

$$k(n) = \left(2^n \sqrt{\pi}^{(n-3)} \frac{\Gamma((3+n)/2)}{2+n} \right)^{1/(1+n)}. \quad (16)$$

The respective form factors for the case of n -dimensions which should be introduced for the parton-level cross section to reproduce the correct cross section from the Lagrangian with contact interactions (14) is

$$FF = (4\pi k(n))^2 \left(\frac{\overline{M}_{PL}}{\sqrt{s}} \right)^{\frac{2n}{1+n}} \Theta(\sqrt{s} - \overline{M}_{PL}). \quad (17)$$

Here the case $n = 0$ corresponds to 4-dimensional models with low scale quantum gravity [3–5], $n = 1$ to Randall Sundrum [2] brane world model¹ and $n \geq 2$ to ADD model [1]. Note that there are astrophysical constraints on $n = 2, 3, 4$ ADD which shift exclude a Planck mass in the few TeV region, it is however interesting to consider bounds from QBHs which are independent of those coming from Kaluza Klein modes which lead to the astrophysical constraints.

II. PHENOMENOLOGY OF THE QBHS AT THE LHC

To study the phenomenology of the QBHs production we have implemented interactions given by Eq.(14-17) into CalcHEP software package [27] as a QBH model which is publicly available at the High Energy Physics Model Database (HEPMDB) [28] under the link <http://hepmdb.soton.ac.uk/hepmdb:1113.0146>. We also would like to note an important feature of CalcHEP which allows the implementation of non-trivial form factors at the user level which was one of the key points in the implementation of this model. We emphasise that the Lagrangian we are proposing to describe the interactions of quantum black holes with particles of the Standard Model should not be regarded as an effective theory in the usual sense, it is rather an effective manner to describe the interactions of these black holes with usual particles.

¹ Note that will treat the Randall Sundrum quantum black holes as ADD ones with $n = 1$. While the cross section for semi-classical black holes in the case of RS differs from that obtained using the Schwarzschild metric [19], this is an unnecessary refinement for quantum black holes whose quantum geometry is anyway very poorly understood.

This model is publicly available at HEPMDB which provides HEP community with a new QBH Monte-Carlo (MC) generator (QBH@HEPMDB), and is an alternative to existing BlackMax [9] and QBH [29] MC generators. We would like to stress that QBH@HEPMDB model is available for download and allows (at HEPMDB website or using CalcHEP locally) to evaluate cross sections and generate parton-level events in generic Les Houches Event (LHE) format [30] which can be *independently* used in subsequent analysis using various general purpose MC generators and detector simulation software. In this paper we present the first phenomenological application of the QBH@HEPMDB model with spin-0 neutral QBH [QBH(0,0)] to e^+e^- and $e\mu$ signature at the LHC@8TeV and LHC@13TeV. We produce the respective projections for the LHC to probe QBH parameter space. The model can be easily extended for QBHs with other charges and spins using the same approach as described above. In our calculations we have used CTEQ6L[31] parameterisation for the parton density functions (PDFs) while the QCD scale was fixed to \overline{M}_{PL} . The parameter space of the model under study is the reduced Planck mass, \overline{M}_{PL} , which sets the threshold for the QBH production as well the number of the extra-dimensions n .

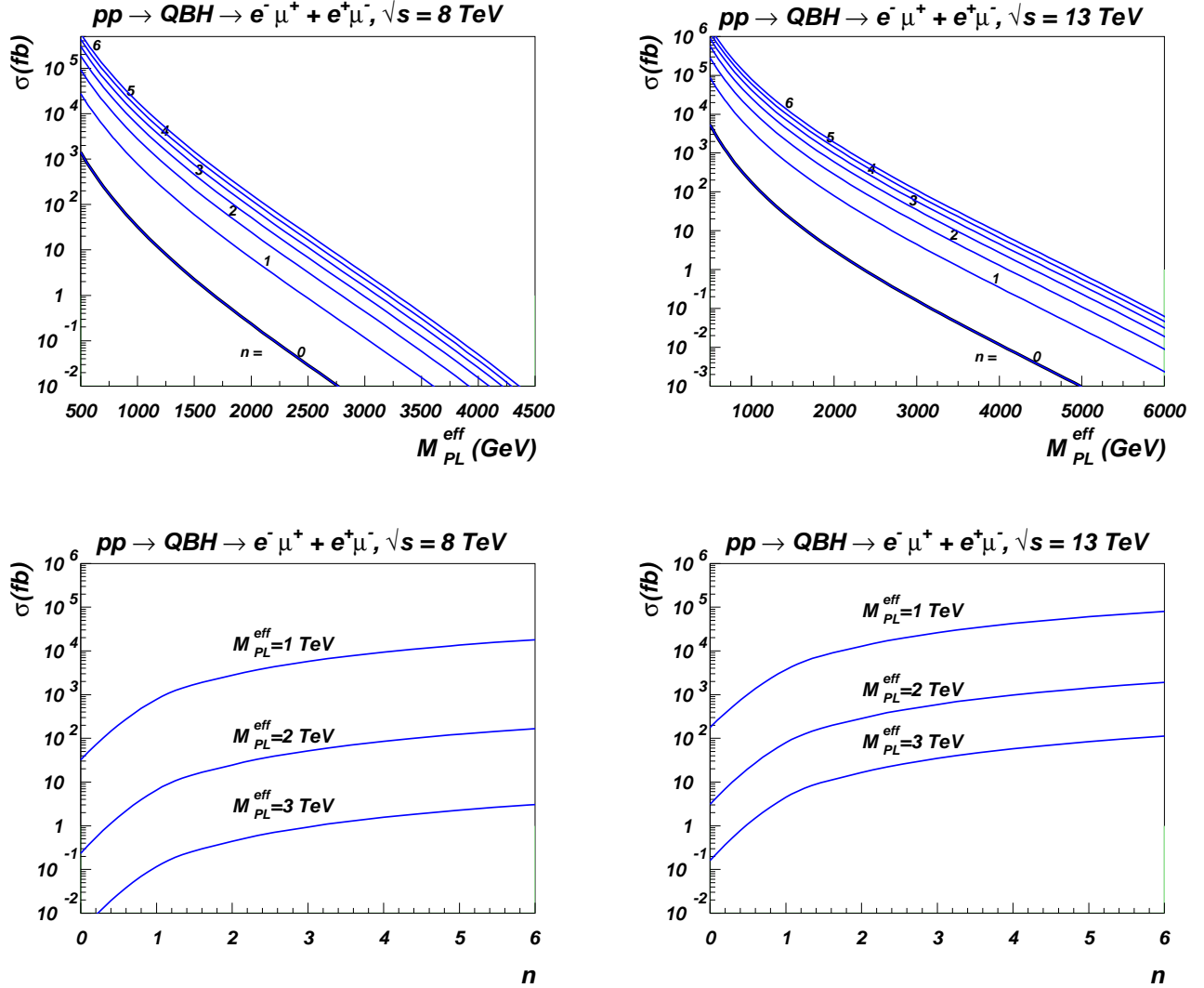


FIG. 1: The cross section of $pp \rightarrow QBH(0,0) \rightarrow e^-\mu^+ (+e^+\mu^-)$ process at the LHC for 8 TeV (left) and 13 TeV (right) centre-of-mass energy pp collisions. Upper row: cross section versus \overline{M}_{PL} , bottom row: cross section versus n .

We start by presenting the QBH production cross section in Fig. 1 where the cross section versus \overline{M}_{PL} (upper row) and versus n (bottom row) is given for $pp \rightarrow QBH(0,0) \rightarrow e^-\mu^+ (+e^+\mu^-)$ process at the LHC for 8 TeV (left) and 13 TeV (right) centre-of-mass energy pp collisions. The respective specific numbers for the cross section are given in Table I. Note that the cross section for $pp \rightarrow QBH(0,0) \rightarrow e^-e^+$ production is a factor of two smaller because of the respective QBH branching ratio. One can observe a big difference in cross sections between effective four-dimensional

	\overline{M}_{PL} (TeV)	n=0	n=1	n=2	n=3	n=4	n=5	n=6
LHC@8TeV	1.0	32.3	782.	2760.	5730.	9370.	13500.	18100.
	2.0	0.235	6.60	24.5	51.8	85.7	124.	166.
	3.0	0.00388	0.116	0.439	0.939	1.56	2.28	3.06
LHC@13TeV	1.0	177.	373.	12800.	26000.	42200.	60500.	80400.
	2.0	3.11	79.7	286.	596.	980.	1420.	1890.
	3.0	0.161	4.48	16.5	34.8	57.4	83.5	112.

TABLE I: The cross section for $pp \rightarrow QBH(0,0) \rightarrow e^- \mu^+ (+e^+ \mu^-)$ process at the LHC in fb for 8 TeV and 13 TeV centre-of-mass energy pp collisions for $\overline{M}_{PL}=1,2,3$ TeV and $n=1-6$.

case ($n = 0$) and higher dimensional theories, for which the cross section of QBH production can be three orders of magnitude higher as, for example, for $n = 6$ case, when the cross section driven by the factor (17). The cross section dependence as a function of n is explicitly presented in the bottom row of Fig. 1 for three fixed values of $\overline{M}_{PL} = 1, 2, 3$ TeV. One can note that the steep cross section drop as a function of \overline{M}_{PL} is defined by PDFs and reaches 0.1 fb around $\overline{M}_{PL} = 2$ TeV for $n = 0$ and around $\overline{M}_{PL} = 4$ TeV for $n = 6$ at the LHC@8TeV. At the LHC@13TeV the cross section reaches 0.1 fb around $\overline{M}_{PL} = 3$ TeV for $n = 0$ and around $\overline{M}_{PL} = 6$ TeV for $n = 6$. Let us note that 0.1 fb cross section level is the typical sensitivity which is expected at 20 fb^{-1} at LHC@8TeV or 30 fb^{-1} at LHC@13TeV (first year run) luminosities providing respectively few events which under assumption of the negligible background allows to establish exclusion at the 95% CL. It is worth discussing the *shape* of the kinematical distributions from QBH(0,0) decay products. In Fig. 2 we present $e\mu$ invariant mass distribution for different n for LHC for 8 TeV (left) and 13 TeV (right) and $\overline{M}_{PL} = 1$ (left) and 2 TeV (right). Results are presented for the same normalisation to compare the shapes of the distributions for different n . The signal shape exhibits a threshold production nature and driven primarily by steeply falling PDFs. It is qualitatively different from a Breit-Wigner shape of resonances, e.g. Z' bosons, appearing in various BSM models different from QBH ones. One can observe the shape difference between different extra-dimensional models and the effective four-dimensional theory. Moreover, the more phase space is available, the bigger difference in the high invariant mass tail which drops faster for larger number of extra dimensions. This is actually what one can expect recalling the energy dependent nature of the form-factor given by Eq.(17). So, $n = 0^2$ distributions has the slowest $M_{e\mu}$ dependence which sharpens with the increase of n driven by Eq.(17). One can see that in the large n limit the parton level asymptotically becomes less and less s dependent, so $M_{e\mu}$ distributions become similar and are defined by rapidly falling PDFs. One should also note that all $M_{e\mu}$ distributions, exhibit a clear step at the QBH production threshold and are qualitatively different from the resonant Breit-Wigner shape. Therefore in our analysis of the LHC sensitivity to the QBH parameter space, we set a lower $M_{e\mu}$ cut rather than a mass-window cut.

Lets turn now to p_T^ℓ distribution presented in Fig. 3. One can see that the difference between transverse momentum distributions is clearly connected with s dependence of Eq.(17) and eventually correlated with differences in $M_{e\mu}$ distributions. At the same time it is worth noting that the difference in the high energy tail distribution will not visibly affect acceptance/selection cuts as we discuss below. Finally lets take a look at the pseudorapidity distributions in bottom left frame of Fig. 4 which demonstrate that η_ℓ distributions are very similar for the scenarios with different n . Looking at Fig.2-4 one can conclude that in spite of the differences for certain kinematical distributions for different n for high values of $M_{\mu e}$ and $P_T^{e,\mu}$, one can expect a very similar acceptance efficiency for these models, since all of them provide high P_T leptons (with P_T far above the acceptance cuts) with a very similar rapidity distributions.

We have also performed signal vs background analysis for the QBH(0,0) production at the LHC decaying into e^+e^- and $e\mu$ final states. The main backgrounds for the e^+e^- signature are $pp \rightarrow e^+e^-$ Drell-Yan (DY) process, as well as $\bar{t}t$ and W^+W^- pair production. The rate of these backgrounds together with the signal rate for $\overline{M}_{PL} = 0.5, 1$ and 2 TeV is presented in Fig. 5(left) for $M_{e^+e^-}$ invariant mass distribution. The QBH signal is shown for $n = 0$ case. One can see the dominant DY background is below the signal, but non negligible for not very high QBH masses. At the same time DY background is absent in case $e\mu$ signature, as shown in Fig. 5(right). One can also see that in case of this signature $\bar{t}t$ and W^+W^- backgrounds are negligible, so LHC potential to probe this signature purely depends on the signal rate which is defined by \overline{M}_{PL} and n parameters. Analogous distributions are presented in Fig. 6 for

² Note that the limit for $n = 0$ obtained here does apply to the specific models described in [3–5] since these models have large hidden sectors and neutral quantum black holes would decay massively in the particles of the hidden sector. However, charged black holes, which are not considered here, would decay into standard model particles.

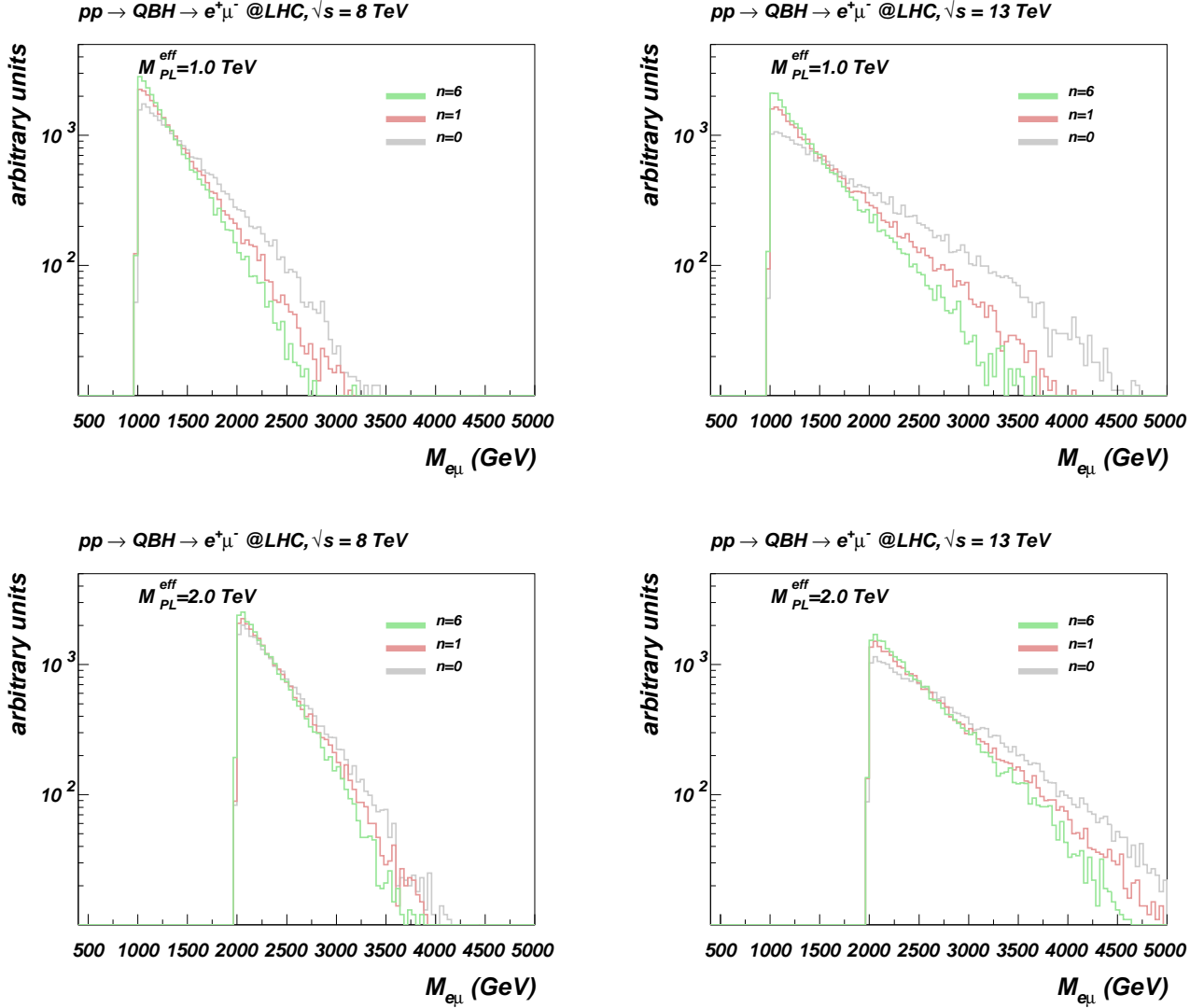


FIG. 2: Invariant mass of $e\mu$ distribution for different n for LHC for 8 TeV (left) and 13 TeV (right) and $\overline{M}_{PL} = 1$ (left) and 2 TeV (right). Results are presented with the same normalisation

LHC@13 TeV exhibiting qualitatively the same pattern for signal and backgrounds for the e^+e^- and $e\mu$ signatures under study.

At the final step we estimate sensitivity of the LHC@8 and 13 TeV to the signatures from QBH under study and estimate the respective limits in case if signal is not observed. In our analysis though we restrict ourselves to the study at parton-level and do take into account realistic electromagnetic energy resolution, using a value of $0.15/\sqrt{E(\text{GeV})}$, which is typical for the ATLAS and CMS detectors and require $|\eta_{\mu,e}| < 2.5$ and $p_T^{e,\mu}$ with respect to the acceptance cuts. We also suggest the simple analysis cut to be $M_{e\mu}(M_{ee}) > 1.1 \times \overline{M}_{PL}$, noting that the acceptance efficiency will be very similar for different n models. In Fig. 7 we present the signal significance for QBH signatures under study at the LHC. For both criteria, exclusion and discovery, we use the following formula for statistical signal significance α as [32]

$$\alpha = 2(\sqrt{N_S + N_B} - \sqrt{N_B}) \quad (18)$$

and require $\alpha \geq 2$ for exclusion region and $\alpha \geq 5$ for the discovery region. The $N_{S(B)} = \sigma_{S(B)}\mathcal{L}$ denotes the number of signal (background) events for an integrated luminosity \mathcal{L} . The figure presents results for LHC@8 (20 fb^{-1}) and 13 TeV (30 fb^{-1}) for $n = 0$ and 6 as two extreme cases for the range of n under study. The

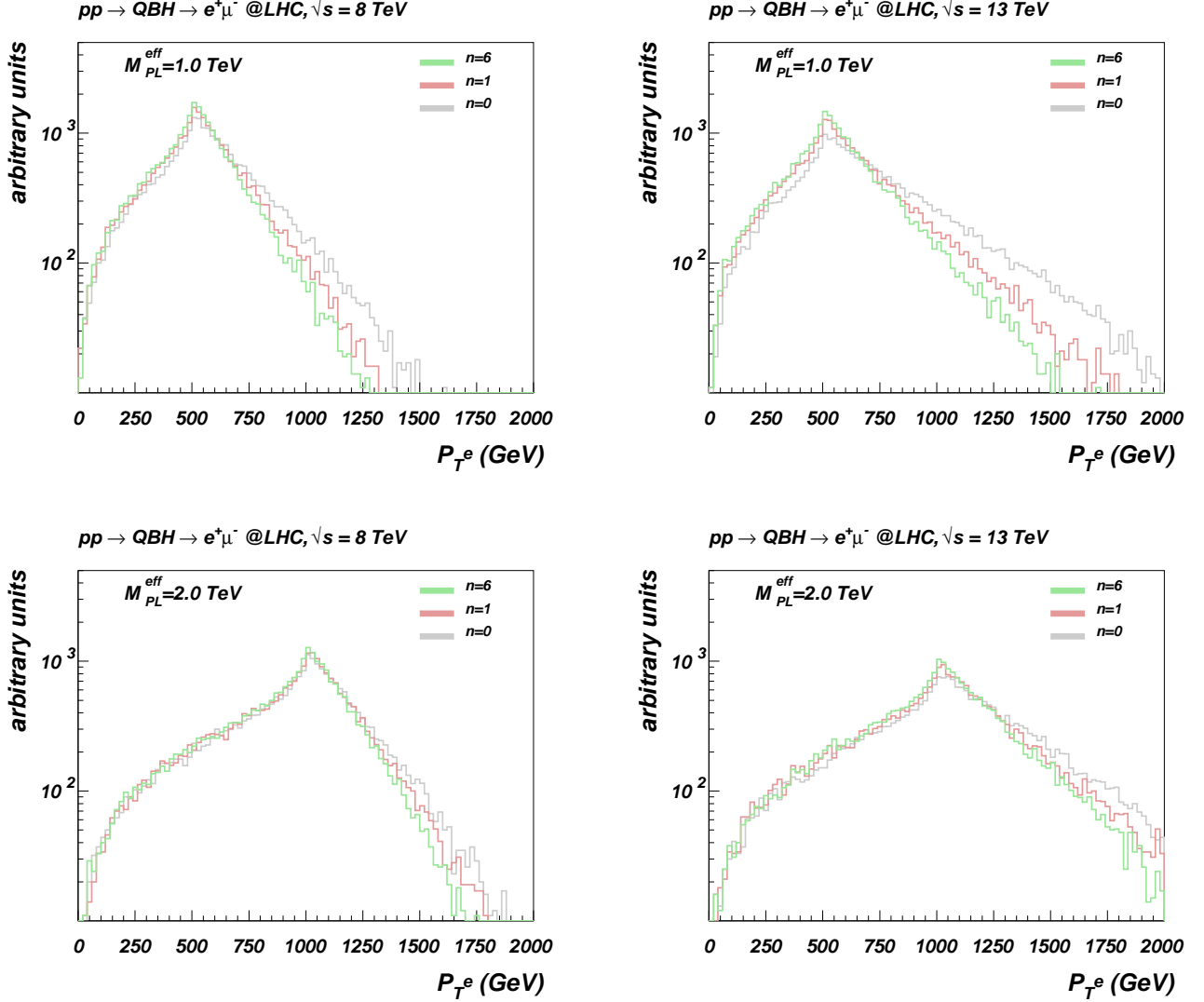


FIG. 3: p_T^e distribution for different n for LHC for 8 TeV (left) and 13 TeV (right) and $\overline{M}_{PL} = 1$ (left) and 2 TeV (right). Results are presented for the same normalisation

The respective \overline{M}_{PL} exclusion and discovery limits for LHC@8 and 13 TeV for $n = 0$ and $n = 6$ scenarios are presented in Table II. One can see that for $n = 0$ the LHC@8TeV the limit on \overline{M}_{PL} @95% CL is only about 1.92 TeV for e^+e^- signature and 2.24 TeV for $e\mu$ one, while the respective discovery numbers are 1.55 and 1.81 TeV respectively. The LHC@13TeV in the first year will be able to improve limits and cover \overline{M}_{PL} @95% CL up to 3.36 TeV with e^+e^- signature and up to 3.78 TeV with $e\mu$, and discover QBH with \overline{M}_{PL} up to 2.79 and 3.18 TeV respectively. At the same time the for $n = 6$ for which the QBH production cross section is about 3 orders of magnitude higher, the LHC reach is much more impressive. For example, with $e\mu$ signature LHC@8 will be able to exclude $\overline{M}_{PL} < 3.68$ TeV @95% CL or discover QBH with $\overline{M}_{PL} < 3.30$ TeV. Analogous numbers for LHC@13TeV are even more exciting – it would be able to probe $\overline{M}_{PL} < 5.75$ TeV or discover the $e\mu$ signal for $\overline{M}_{PL} < 5.10$ TeV. It is worth noting that though our analysis reproduces quite well recent ATLAS results on QBH search at LHC@8TeV [33], which stated the 3.65 TeV limit for $n = 6$ case for $e^+e^- + \mu^+\mu^-$ signatures. Since the signal cross section for this signature equal to the cross section for the $e\mu$ signal while background is negligible, the limits are expected to be the same for both cases. The respective limit from our study is 3.67 TeV which is in a very good agreement with the above one from ATLAS. We should also mention that the signal cross section, quoted by [33] for $n = 6$ case agrees within 10% with the cross section we found in our paper. Therefore we can also conclude about the successful validation of our generator and

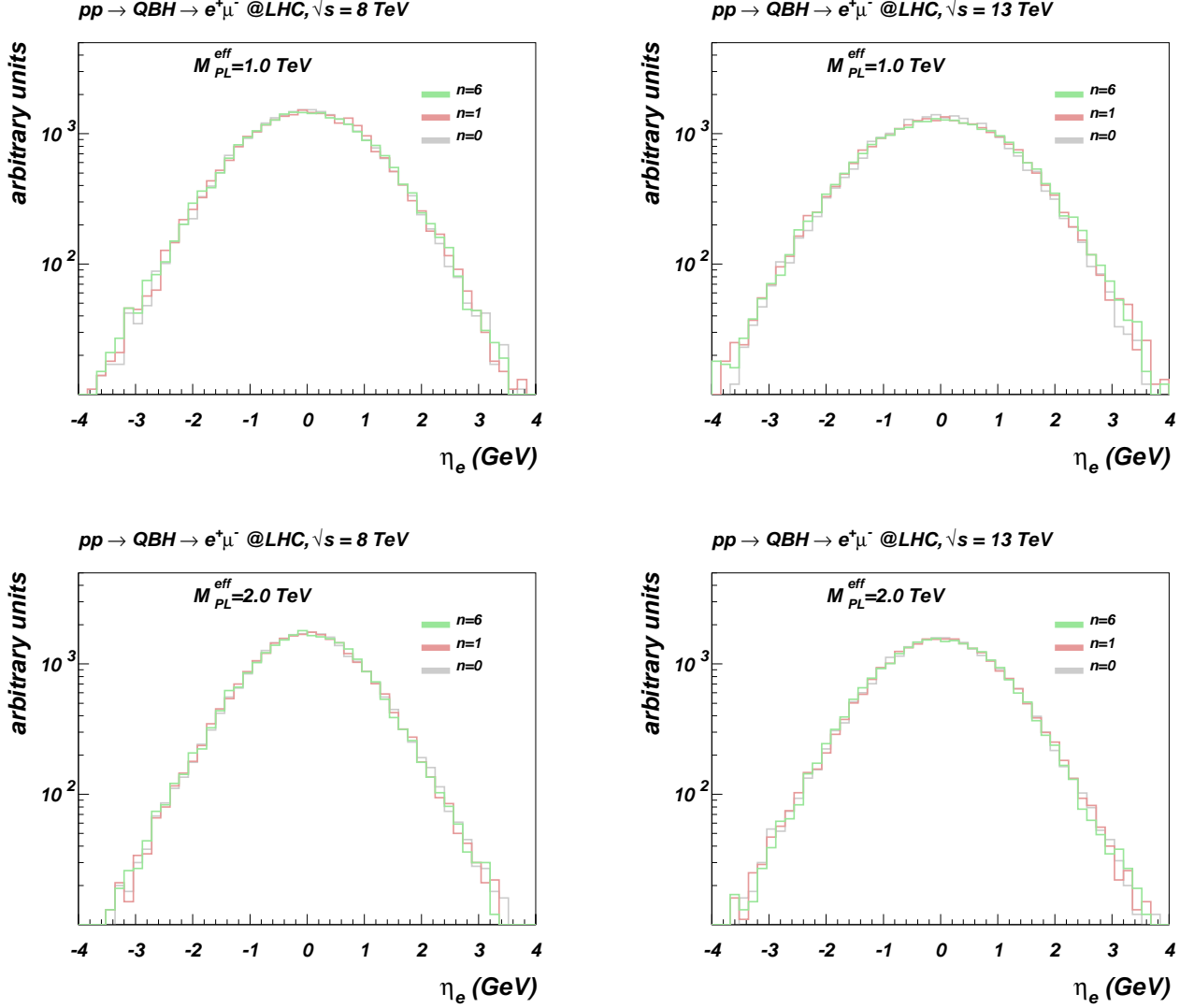


FIG. 4: Pseudorapidity of lepton distribution for different n for LHC for 8 TeV (left) and 13 TeV (right) and $\overline{M}_{PL} = 1$ (left) and 2 TeV (right). Results are presented for the same normalisation

analysis for the LHC@8TeV.

III. CONCLUSIONS

We discuss a field theoretical framework to describe the interactions of non-thermal QBH with particles of the Standard Model and propose a non-local Lagrangian to describe the production of these QBH which is designed to reproduce the geometrical cross section πr_s^2 for black hole production. We have implemented this model into CalcHEP and it is publicly available at the High Energy Model Database for simulation of QBH events at the LHC and future colliders. This model, QBH@HEPMDB is an effective independent tool for QBH phenomenological and experimental explorations. Detailed comparison of QBH@HEPMDB with analogous tools on the market requires dedicated work which we plan to perform in the nearest future. In this paper we present the first phenomenological application of the QBH@HEPMDB model with spin-0 neutral QBH giving rise the e^+e^- and $e\mu$ signatures at the LHC@8TeV and LHC@13TeV and produce the first respective projections in terms of limits on the reduced Planck mass, \overline{M}_{PL} and the number of the extra-dimensions n . In particular we found that among two signatures, $e\mu$ one

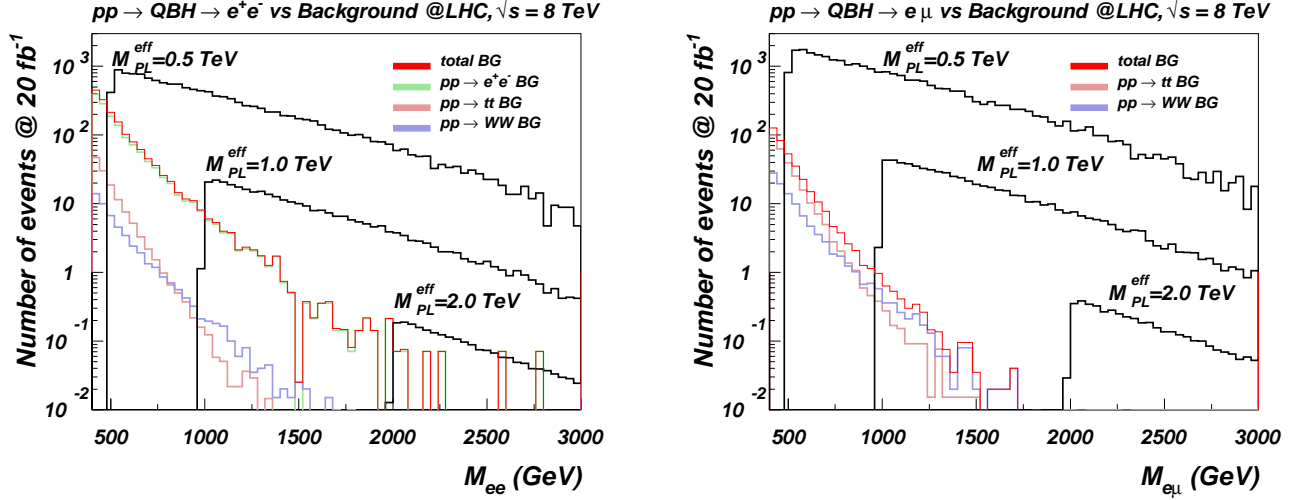


FIG. 5: Invariant mass distributions for e^+e^- (left) and $e\mu$ (right) QBH signatures ($n = 0$ case) and the respective backgrounds for LHC@8TeV

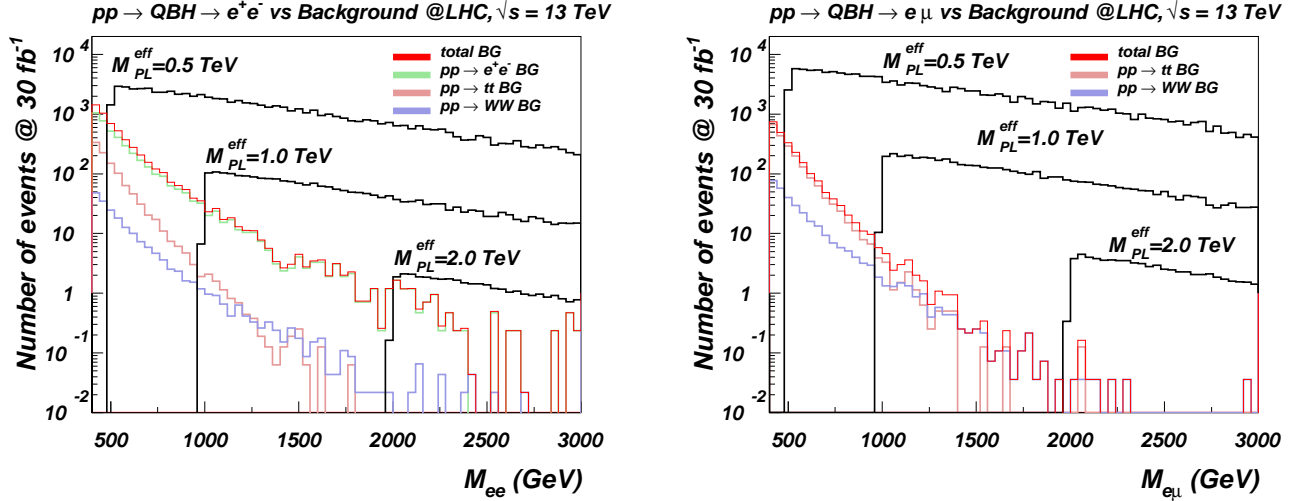


FIG. 6: Invariant mass distributions for e^+e^- (left) and $e\mu$ (right) QBH signatures ($n = 0$ case) and the respective backgrounds for LHC@13TeV

provides the best LHC reach since it is free of DY background. We have successfully validated our generator and exclusion limits against recent ATLAS results for $n = 6$ case. We found that with $e\mu$ signature, for number of extra-dimensions, n , in the range of 0-6, the LHC@8 will be able to probe the respective range of 2.2-3.7 TeV of the reduced Planck Mass \bar{M}_{PL} . We have also produced new projections for LHC@13 and found that even in the first year of operation with 30fb^{-1} the range 3.8-5.8 TeV of \bar{M}_{PL} at 95%CL can be probed. The respective discovery range of LHC@13 is 3.2-5.1 TeV for \bar{M}_{PL} .

Acknowledgements: We are grateful to Tim Morris, Alexander Pukhov, Claire Shepherd-Themistocleous, Emmanuel Olaiya, Andreas Gueth and Thomas Reis for stimulating discussions. This work is supported in part by the European Cooperation in Science and Technology (COST) action MP0905 “Black Holes in a Violent Universe” and by the Science and Technology Facilities Council, grants number ST/L000504/1 and ST/L000296/1.

		LHC@8TeV		LHC@13TeV	
CL	n	e^+e^-	$e\mu$	e^+e^-	$e\mu$
95%CL	0	1920 GeV	2240 GeV	3360 GeV	3780 GeV
5σ	0	1550 GeV	1810 GeV	2790 GeV	3180 GeV
95%CL	6	3540 GeV	3680 GeV	5510 GeV	5750 GeV
5σ	6	3140 GeV	3300 GeV	4850 GeV	5100 GeV

TABLE II: \overline{M}_{PL} exclusion and discovery limits for LHC@8 and 13 TeV for $n = 0$ and $n = 6$ scenarios.

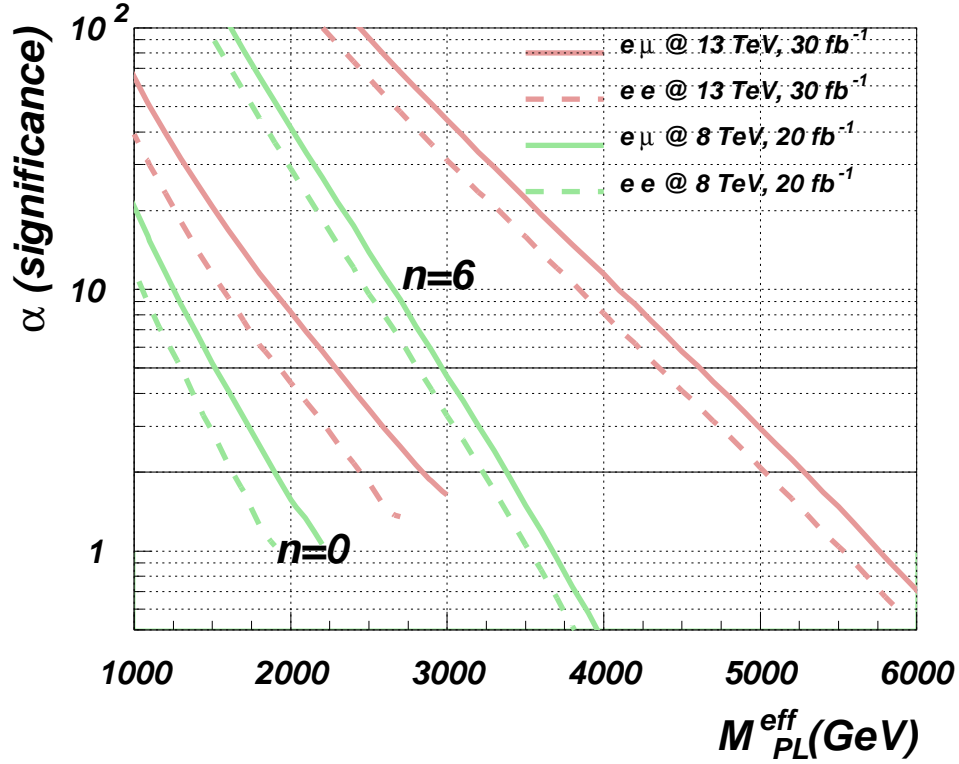


FIG. 7: Signal significance for QBH e^+e^- and $e\mu$ signatures as a function of \overline{M}_{PL} for $n = 0$ and 6 at the LHC@8 and 13 TeV.

-
- [1] N. Arkani-Hamed, S. Dimopoulos, G. R. Dvali, Phys. Lett. **B429**, 263-272 (1998) [hep-ph/9803315]; I. Antoniadis, N. Arkani-Hamed, S. Dimopoulos *et al.*, Phys. Lett. **B436**, 257-263 (1998) [hep-ph/9804398].
- [2] L. Randall, R. Sundrum, Phys. Rev. Lett. **83**, 3370-3373 (1999) [hep-ph/9905221].
- [3] X. Calmet, S. D. H. Hsu, D. Reeb, Phys. Rev. **D77**, 125015 (2008) [arXiv:0803.1836 [hep-th]].
- [4] X. Calmet, Mod. Phys. Lett. A **25**, 1553 (2010) [arXiv:1005.1805 [hep-ph]].
- [5] X. Calmet, arXiv:1410.2807 [hep-th].
- [6] S. Dimopoulos and G. L. Landsberg, Phys. Rev. Lett. **87**, 161602 (2001) [arXiv:hep-ph/0106295].
- [7] T. Banks and W. Fischler, arXiv:hep-th/9906038.
- [8] S. B. Giddings and S. D. Thomas, Phys. Rev. D **65**, 056010 (2002) [arXiv:hep-ph/0106219].
- [9] D. -C. Dai, G. Starkman, D. Stojkovic, C. Issever, E. Rizvi and J. Tseng, Phys. Rev. D **77**, 076007 (2008) [arXiv:0711.3012 [hep-ph]].
- [10] X. Calmet, W. Gong, S. D. H. Hsu, Phys. Lett. **B668**, 20-23 (2008) [arXiv:0806.4605 [hep-ph]].

- [11] J. L. Feng and A. D. Shapere, Phys. Rev. Lett. **88**, 021303 (2002) [arXiv:hep-ph/0109106].
- [12] L. A. Anchordoqui, J. L. Feng, H. Goldberg and A. D. Shapere, Phys. Lett. B **594**, 363 (2004) [arXiv:hep-ph/0311365].
- [13] L. A. Anchordoqui, J. L. Feng, H. Goldberg and A. D. Shapere, Phys. Rev. D **65** (2002) 124027 [arXiv:hep-ph/0112247].
- [14] L. A. Anchordoqui, J. L. Feng, H. Goldberg and A. D. Shapere, Phys. Rev. D **68**, 104025 (2003) [arXiv:hep-ph/0307228].
- [15] X. Calmet and M. Feliciangeli, Phys. Rev. D **78**, 067702 (2008) [arXiv:0806.4304 [hep-ph]].
- [16] X. Calmet, L. I. Caramete and O. Micu, JHEP **1211**, 104 (2012) [arXiv:1204.2520 [hep-ph]].
- [17] N. Arsene, X. Calmet, L. I. Caramete and O. Micu, Astropart. Phys. **54**, 132 (2014) [arXiv:1303.4603 [hep-ph]].
- [18] X. Calmet, B. Carr and E. Winstanley, “Quantum Black Holes, ” Springer Briefs in Physics, ISBN-10: 3642389384, ISBN-13: 978-3642389382, Springer, Edition: 2013.
- [19] P. Meade and L. Randall, JHEP **0805**, 003 (2008) [arXiv:0708.3017 [hep-ph]].
- [20] D. M. Eardley and S. B. Giddings, Phys. Rev. D **66**, 044011 (2002) [arXiv:gr-qc/0201034];
- [21] P. D. D’Eath and P. N. Payne, Phys. Rev. D **46**, 658 (1992); Phys. Rev. D **46**, 675 (1992); Phys. Rev. D **46**, 694 (1992).
- [22] S. D. H. Hsu, Phys. Lett. B **555**, 92 (2003) [arXiv:hep-ph/0203154].
- [23] X. Calmet, D. Fragkakis and N. Gausmann, Eur. Phys. J. C **71**, 1781 (2011) [arXiv:1105.1779 [hep-ph]]; “Non thermal small black holes,” chapter 8 in A.J. Bauer and D.G.Eiffel editors, Black Holes: Evolution, Theory and Thermodynamics Nova Publishers, New York, 2012, arXiv:1201.4463 [hep-ph].
- [24] X. Calmet and N. Gausmann, Int. J. Mod. Phys. A **28**, 1350045 (2013) [arXiv:1209.4618 [hep-ph]].
- [25] X. Calmet, “Fundamental Physics with Black Holes,” chapter 1 of Quantum Aspects of Black Holes, X. Calmet (Ed.), volume 178 of the series Fundamental Theories of Physics, Springer, 2015, ISBN 978-3-319-10851-3.
- [26] D. M. Gingrich, J. Phys. G **37**, 105008 (2010) [arXiv:0912.0826 [hep-ph]].
- [27] A. Belyaev, N. D. Christensen and A. Pukhov, Comput. Phys. Commun. **184**, 1729 (2013) [arXiv:1207.6082 [hep-ph]].
- [28] M. Bondarenko, A. Belyaev, L. Basso, E. Boos, V. Bunichev *et al.*, “High Energy Physics Model Database : Towards decoding of the underlying theory” (within “Les Houches 2011: Physics at TeV Colliders New Physics Working Group Report”), arXiv:1203.1488 [hep-ph], <https://hepmdb.soton.ac.uk>
- [29] D. M. Gingrich, Comput. Phys. Commun. **181**, 1917 (2010) [arXiv:0911.5370 [hep-ph]].
- [30] J. Alwall, A. Ballestrero, P. Bartalini, S. Belov, E. Boos, A. Buckley, J. M. Butterworth and L. Dudko *et al.*, Comput. Phys. Commun. **176**, 300 (2007) [hep-ph/0609017].
- [31] J. Pumplin, D. R. Stump, J. Huston, H. L. Lai, P. M. Nadolsky and W. K. Tung, JHEP **0207**, 012 (2002) [hep-ph/0201195].
- [32] S. I. Bityukov and N. V. Krasnikov, Nucl. Instrum. and Methods, **A452**, pp 518-524 (2000)
- [33] G. Aad *et al.* [ATLAS Collaboration], Phys. Rev. D **90**, 052005 (2014) [arXiv:1405.4123 [hep-ex]].